

## Vortex tube models for turbulent dynamo action

Alberto Bigazzi

*Department of Mathematics, University of Newcastle upon Tyne, NE1 7RU, United Kingdom  
and Dipartimento di Fisica, Università dell'Aquila, I-67100 Coppito, L'Aquila, Italy*

Axel Brandenburg<sup>a)</sup>

*Department of Mathematics, University of Newcastle upon Tyne, NE1 7RU, United Kingdom*

David Moss

*Department of Mathematics, The University, Manchester M13 9PL, United Kingdom*

(Received 30 June 1998; accepted 22 September 1998)

The possibility of dynamo action resulting from a pair of elongated vortex structures immersed in an electrically conducting fluid is investigated. For elongated vortex structures, the critical magnetic Reynolds number for dynamo action is about half that for the spherical rotors that have been studied previously. When applied to Kolmogorov turbulence with vortex structures of scale comparable to the dissipation length, this model can explain dynamo action only when the magnetic Prandtl number (=kinematic viscosity/magnetic diffusivity) exceeds a critical value that is larger than unity. It is argued that in astrophysical bodies where this condition is not satisfied (in stellar convection zones, for example), dynamo action must instead result from motions on all scales up to the size of the region. © 1999 American Institute of Physics. [S1070-664X(99)01001-0]

### I. INTRODUCTION

Over the last decade, the presence of coherent structures in turbulent flows has been recognized as being a distinctive feature, clearly visible in visualizations of vorticity in hydrodynamical simulations performed by several groups.<sup>1-3</sup> These structures consist of vortex filaments, whose diameter is comparable with the dissipation scale and with length stretching to the integral length scale. The question of the role of this tangle of vortices for the dynamics, and for the statistical properties of the flow has attracted significant attention.<sup>4,5</sup>

In the present paper we address the question of whether the vortex filaments in an electrically conducting fluid might play a direct role in the generation of magnetic fields by means of dynamo action. The generation of small-scale magnetic fields<sup>6,7</sup> has been seen in various turbulence simulations.<sup>8-12</sup> Here we attempt to determine whether the vortex filaments themselves may interact with a seed magnetic field in order to produce small-scale dynamo action.

This study is motivated by recent work simulating dynamo action from two inclined rotors.<sup>13</sup> This type of dynamo was first studied by Herzenberg<sup>14</sup> and, in fact, provided one of the first two rigorous proofs of the existence of dynamo action. The original Herzenberg dynamo consists of two rigidly rotating spheres within a solid body of finite but large extent. The electrical conductivity of rotor and container are the same. In an experimental realization of this model,<sup>15</sup> the rotors were metal cylinders, embedded in a block of the same material, using mercury as a conducting lubricator. The three-dimensional simulations<sup>13</sup> were carried out on a Cartesian mesh using a smoothed velocity field representing the

two rigidly rotating spheres in an electrically conducting medium at rest. Above a certain critical magnetic Reynolds number a weak seed magnetic field begins to grow exponentially. The critical values for dynamo action, as determined numerically, agree well with the asymptotic theory<sup>14</sup> for the Herzenberg dynamo. In the paper of Brandenburg *et al.*,<sup>13</sup> a Herzenberg-type process involving close fluid vortex pairs was also briefly discussed as a possible model for dynamo action.

In the present paper we pursue this suggestion further. First of all we present the results of numerical simulations of a modified Herzenberg-type dynamo, whose geometry is intended to approximate that of a vortex filament. Thus, instead of spherical rotors, we consider the case of elongated ellipsoids, whose major axes are much longer than the other two and lie along the rotation vectors. We find that in this modified geometry the dynamo still operates and, furthermore, the critical magnetic Reynolds number for the onset of dynamo action is smaller, being roughly one half of that of the original Herzenberg model.

Then, we apply those results to test the hypothesis of small-scale dynamo action resulting from the interaction of vortex filaments in turbulent flows. In order to draw a connection between our vortex model and turbulence, we make use of a scaling argument based on the Kolmogorov theory of turbulence. We then finally compare our predictions with data from Brandenburg *et al.*,<sup>12</sup> who simulated convective dynamo action in a rotating box.<sup>12</sup> Those simulations are tailored to represent part of the sun near the bottom of the convection zone. The model is compressible, and overshoot into the stably stratified radiative interior beneath is included. Despite the amount of detailed physics included, the main features of dynamo action agree with earlier simulations for simpler models.<sup>9,10</sup>

<sup>a)</sup>Electronic mail: Axel.Brandenburg@ncl.ac.uk

This paper is organized as follows. In Sec. II we describe our simulations of a kinematic Herzenberg-type rotor dynamo and obtain an estimate for the value of the critical magnetic Reynolds number for the onset of dynamo action in this modified geometry. In Sec. III we make use of Kolmogorov scaling to give an estimate for the conditions under which a Herzenberg-type dynamo, resulting from the interaction of vortex filaments, could be excited in Kolmogorov turbulence. In Secs. IV and V we test the hypothesis of vortex-generated dynamo action, using data from simulations of compressible hydromagnetic convection of Brandenburg *et al.*,<sup>12</sup> in which small-scale dynamo action is observed. We are led to the conclusion that the role of vortex tubes in the generation of small-scale magnetic fields cannot be as straightforward as suggested by Brandenburg *et al.*<sup>13</sup> Therefore we consider in Sec. VI two possible modifications of the mechanism proposed in Sec. II: First, we consider a model with a spherical rotor and a vortex sheet, and subsequently we examine the possible role of vortex clusters in the generation of large-scale magnetic fields.

## II. A HERZENBERG-TYPE DYNAMO

The Herzenberg dynamo consists of two rigidly rotating spheres in a conducting medium. The conductivity is finite, and the same inside and outside the spheres, which have radius  $a$  and are separated by a distance  $2d$ . The magnetic Reynolds number for the Herzenberg dynamo is defined as

$$\text{Hz} \equiv \Omega a^2 / \eta, \tag{1}$$

where  $\Omega$  is the angular velocity of the spheres and  $\eta$  the magnetic diffusivity. For dynamo action to take place this number has to exceed a certain threshold, which is a function of the ratio  $d/a$  and of the angle between the rotation axes. Qualitatively, in this model each rotor winds up a local poloidal field, generates via field line stretching a strong toroidal field that diffuses then to the other rotor, where it acts as a new local poloidal field. In order for a self-excited dynamo to exist, the two axes must not be exactly parallel or perpendicular. In the particular case where the two rotation axes lie in two parallel planes separated by a distance  $2d$  and are tilted with respect to one another by the angle  $\phi$ , there is monotonic (non-oscillatory) dynamo action when  $\phi$  is between  $90^\circ$  and  $180^\circ$  (Refs. 14, 16, 17 and 13),

$$\text{Hz} > \text{Hz}_{\text{crit}} \approx 69(a/d)^{-3} f(\phi)^{-1/2}, \tag{2}$$

where

$$f(\phi) = \cos^2 \phi \sin \phi. \tag{3}$$

For  $|\phi| \leq 90^\circ$  an oscillatory dynamo exists, with a marginal dynamo number that is 3–10 times larger than for the nonoscillatory dynamo present for  $|\phi| \geq 90^\circ$ .

### A. The numerical simulations

With the aim of connecting the Herzenberg mechanism for dynamo action and the interaction of vortex filaments and magnetic fields in turbulent flows, we generalize the geometry of the Herzenberg dynamo by replacing the spheres with ellipsoids with aspect ratio  $b/a > 1$ , where  $a$  and  $b$  are the

minor and major semi-axes, and the latter is also the rotation axis. Thus, when  $b \gg a$ , we will consider the two ellipsoids as a model of a pair of vortex tubes. In this paper, we only consider the case of nonoscillatory dynamo action from pairs of tubes. We note that a more detailed inspection of vortex pairs in hydromagnetic turbulence simulations does indeed seem to suggest that nearby tubes are more nearly antiparallel than parallel. We use a very similar setup to that described in Ref. 13. We consider a medium of uniform conductivity  $\eta$ . A steady velocity field is constructed such that two ellipsoids centered at  $\mathbf{x}_1, \mathbf{x}_2$  with radius  $a$  and major axis  $b$ , separated by a distance  $2d$ , are rigidly rotating with angular velocities  $\Omega_1$  and  $\Omega_2$  given by

$$\Omega_i(\mathbf{x}) = \Omega_i(\mathbf{x}) \hat{\Omega}_i, \quad \hat{\Omega}_{1,2} = (0, \pm \sin \frac{1}{2} \phi, \cos \frac{1}{2} \phi). \tag{4}$$

(We point out that the corresponding Eq. (2) in Ref. 13 contains a misprint; the 1/2-factor was moved outside the sin and cos functions.) In practice, we construct the velocity field as

$$\mathbf{u}(\mathbf{x}) = \sum_{i=1,2} \Omega_i(\mathbf{x}) \times (\mathbf{x} - \mathbf{x}_i), \tag{5}$$

where  $\Omega_{1,2}(\mathbf{x})$ , are two profile functions that tend to zero outside the rotors. We set

$$\Omega_i(\mathbf{x}) = \Omega \exp[-f_i(\mathbf{x})^n], \tag{6}$$

where  $n = 5$  in our simulations and the scalar functions  $f_i$  are given by

$$f_i(\mathbf{x}) = \frac{(\mathbf{x} - \mathbf{x}_i) \times \hat{\Omega}}{a^2} + \frac{(\mathbf{x} - \mathbf{x}_i) \cdot \hat{\Omega}}{b^2}. \tag{7}$$

The evolution of the magnetic field is governed by the linear induction equation

$$\frac{\partial \mathbf{B}}{\partial t} = \nabla \times (\mathbf{u} \times \mathbf{B}) + \eta \nabla^2 \mathbf{B}. \tag{8}$$

In order to ensure the solenoidality condition  $\nabla \cdot \mathbf{B} = 0$  we write  $\mathbf{B} = \nabla \times \mathbf{A}$  and solve numerically the equation for the vector potential  $\mathbf{A}$ ,

$$\frac{\partial \mathbf{A}}{\partial t} = \mathbf{u} \times \mathbf{B} - \eta \nabla \times \mathbf{B} + \nabla \Phi. \tag{9}$$

Adopting the gauge  $\Phi = \eta \nabla \cdot \mathbf{A}$ , we can write

$$\frac{\partial \mathbf{A}}{\partial t} = \mathbf{u} \times (\nabla \times \mathbf{A}) + \eta \nabla^2 \mathbf{A}. \tag{10}$$

Equation (10) is solved in a cartesian box using a compact sixth order scheme in space<sup>18</sup> and third order time stepping.<sup>19</sup> We adopt periodic boundary conditions in the horizontal plane  $(x, y)$  and vertical field conditions at the vertical boundaries, i.e.,  $B_x = B_y = 0$  on  $z = \pm L_z$ . The aspect ratio is  $L_x : L_y : L_z = 1 : 1 : 1$ .

### B. Results

In Fig. 1 we show the behavior of the critical Herzenberg number  $\text{Hz}_{\text{crit}}$ , as a function of  $b/a$ , the aspect ratio of the ellipsoids. For elongated structures with  $b > a$ , the criti-

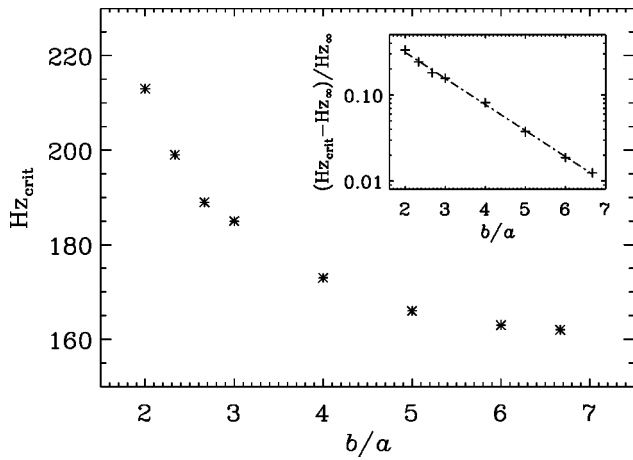


FIG. 1. Behavior of the critical magnetic Reynolds number  $Hz_{crit}$  as a function of  $b/a$  for  $a=0.3$ ,  $d=0.4$  and  $\phi=125^\circ$ . In the inset the same data are plotted on a log-linear scale in the form  $(Hz_{crit} - Hz_\infty)/Hz_\infty$ , where  $Hz_\infty = 160$  is the estimated asymptotic value as  $b/a \rightarrow \infty$ .

cal value of the dynamo number is smaller than for the case  $b=a$  for the same value of  $a$ . For the particular value  $\phi = 125^\circ$ , we find numerically that  $Hz_{crit}$  approaches a limit as  $b/a$  increases (see Fig. 1). In this limit  $Hz_{crit}$  is about half the value for spherical rotors,  $a=b$ . For values of  $\phi$  closer to  $0^\circ$ ,  $90^\circ$  or  $180^\circ$  the critical value is larger, in accordance with Eq. (2).

The fact that the critical value of the dynamo number does not decrease further as  $b/a$  increases can be explained if we note that dynamo action originates from the interaction of magnetic fields in those regions where the separation of the vortices is smallest. The size of these regions does not vary as  $b/a$  increases beyond a certain critical value, for any given orientation. Also, the field twisting and stretching will be most effective near the equatorial regions of the vortices. A vector plot of the field structure, when the dynamo is excited, for the case when  $b/a=6$ , is given in Fig. 2. The

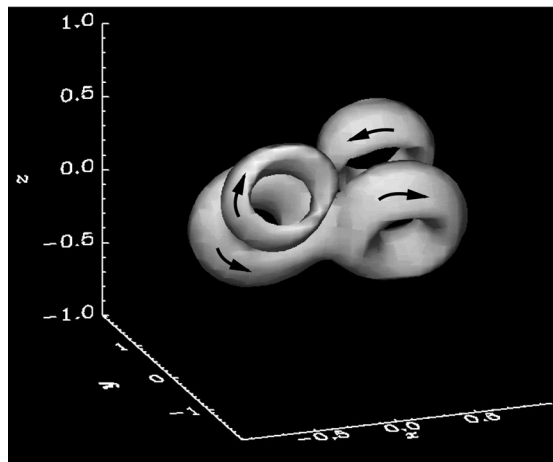


FIG. 2. Three dimensional visualization of the level surface of the magnetic field where  $B^2=1.3$ , which corresponds to 45% of the maximum field strength. The orientation of the magnetic field is indicated by arrows.  $\phi = 125^\circ$ ,  $b = 1.8$ ,  $a = 0.3$ ,  $d = 0.4$ ,  $Hz = 180$ . Note that the field is concentrated about a central region around the two elongated rotors, where the interaction is largest.

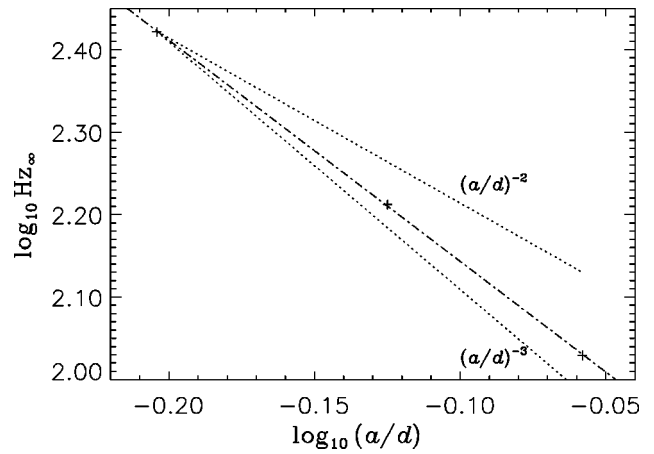


FIG. 3. The critical Reynolds number  $Hz_\infty$  as a function of  $a/d$ , for  $\phi = 125^\circ$ ,  $b = 1.8$ ,  $d = 0.4$ .  $a$  is varied and takes the values 0.25;0.30;0.35. The dotted lines give quadratic ( $m = -2$ ) and cubic ( $m = -3$ ) scalings for comparison.

resulting field looks similar to that in the case of spherical rotors,  $a=b$ , see Ref. 13, indicating that the elongated shape of the rotors has only a weak effect on the resulting field structure.

The behavior of the asymptotic critical value  $Hz_{crit}$  as a function of  $a/d$  is shown in Fig. 3 for the case  $\phi=125^\circ$ . Extrapolating from the figure, we obtain the scaling for the critical asymptotic value,

$$\lim_{b \rightarrow \infty} Hz_{crit} \equiv Hz_\infty = C \times (a/d)^{-2.7}, \tag{11}$$

which is similar to that of Eq. (2). Here  $C$  is a function of  $\phi$  and, possibly,  $a/d$ ; for  $\phi = 125^\circ$  and  $a/d = 0.75$  we have  $C \approx 75$ .

### III. THE HERZENBERG-TYPE DYNAMO IN TURBULENT FLOWS

We have already mentioned that vortex tubes, as seen in numerical simulations, have a typical length much greater than their radius. So we use Eq. (11) to estimate the critical Herzenberg number  $Hz_{crit}$  for a pair of vortex tubes. We define the Herzenberg number  $Hz$  for such a pair in a fashion analogous to (1),

$$Hz = \Omega a^2 / \eta = \omega a^2 / 2\eta, \tag{12}$$

where the angular velocity  $\Omega$  is set at half the value of the vorticity  $\omega$  at the center of the tube. Thus expression (12) for the Herzenberg number only contains quantities that can be related to the properties of the flow. The size of the vortex,  $a$ , and the magnitude of the vorticity  $\omega$ , both depend on the Reynolds number of the flow  $Re$ . If the scaling of those quantities with  $Re$  is known we can calculate the scaling of  $Hz$ . In the following we shall assume that Kolmogorov scaling holds for all the quantities related to the flow. The Reynolds number  $Re$  is defined in the usual way as  $Re = UL/\nu$ , where  $U$  is the rms velocity  $\langle \mathbf{u}^2 \rangle^{1/2}$ ,  $L$  the integral scale of the flow, and  $\nu$  the kinematic viscosity.

### A. Scaling for the tube radius $a$

In order to establish the scaling law for the diameter of the vortex tubes  $a$  in (12), we have to relate this quantity to other characteristic scales in the flow whose scaling law is known from the theory. This is in fact a topic over which debate is still open (see, e.g., Ref. 20) and we thus make use in the following of the two most recurrent hypotheses, namely that

$$a = \ell \text{ or } a = \lambda, \quad (13)$$

$\ell$  is the dissipation scale and  $\lambda$  is the Taylor microscale, defined as

$$\lambda = \sqrt{5\langle \mathbf{u}^2 \rangle / \langle \boldsymbol{\omega}^2 \rangle}, \quad (14)$$

where angular brackets indicate volume averages. In Kolmogorov turbulence,  $\ell$  scales with the Reynolds number as

$$\ell = L \text{Re}^{-3/4}, \quad (15)$$

while  $\lambda$  scales with  $\text{Re}$  like

$$\lambda = L \text{Re}^{-1/2}. \quad (16)$$

These relations assume a Kolmogorov spectrum for the kinetic energy,  $E(k) \sim k^{-5/3}$ . While the relation (15) is well known, we want to briefly sketch a derivation for Eq. (16). If we calculate the mean square value of the vorticity, we have

$$\langle \boldsymbol{\omega}^2 \rangle = \int k^2 E(k) dk \sim k_{\max}^{4/3}, \quad (17)$$

since  $k_{\max} = 2\pi/\ell$ , we find from Eq. (15) that  $\langle \boldsymbol{\omega}^2 \rangle \sim \text{Re}$ . This, together with the definition (14), leads to Eq. (16).

### B. The scaling of Hz with Re

The scaling law for  $\omega$  in (12) is obtained by putting  $\omega a/2 \equiv \Omega a = u_a$  where  $u_a$  is a typical velocity at scale  $a$ . In Kolmogorov turbulence the scaling

$$u_a = U(a/L)^{1/3} \quad (18)$$

holds. Dropping factors of order unity, as elsewhere in this scaling argument, we thus obtain from Eqs. (12), (15), (16) and (18) that

$$\text{Hz} = \frac{UL}{\eta} \left( \frac{\ell}{L} \right)^{4/3} = \text{Pr}_M \text{ (case I)}, \quad (19)$$

and

$$\text{Hz} = \frac{UL}{\eta} \left( \frac{\lambda}{L} \right)^{4/3} = \text{Re}^{1/3} \text{Pr}_M \text{ (case II)}, \quad (20)$$

in the two cases where  $a$  scales either with  $\ell$  or with  $\lambda$ . Here,  $\text{Pr}_M = \nu/\eta$  is the magnetic Prandtl number ( $\nu$  and  $\eta$  are the kinematic and magnetic diffusivities).

Thus we see that, in the first case, the magnetic Reynolds number of a Herzenberg-type dynamo made of a pair of vortex tubes depends *not* on the Reynolds number of the flow, but just on its magnetic Prandtl number. A criterion of this type was first suggested by Batchelor<sup>21</sup> using a qualitative argument based on the similarity between the equations governing magnetic field and vorticity.

TABLE I. Parameters of Runs A and D.  $\omega$  and  $U$  are given in nondimensional units, where  $g=L=1$ .

	Run A	Run D
Mesh	63 <sup>3</sup>	126 <sup>2</sup> × 105
Box extent: $L_x \times L_y \times L_z$	2 × 2 × 2	2 × 2 × 1.65
$L$	1	1
Re	310	1200
$\text{Pr}_M$	4.0	0.5
$\langle \mathbf{u}^2 \rangle^{1/2} \equiv U$	0.065	0.036
$\langle \boldsymbol{\omega}^2 \rangle^{1/2}$	0.74	0.78
$\ell = L \text{Re}^{-3/4}$ , Eq. (15)	0.013	0.005
$\lambda = \sqrt{5} U / \langle \boldsymbol{\omega}^2 \rangle^{1/2}$ , Eq. (14)	0.20	0.10

In the second case, there is the possibility that the critical Herzenberg number for dynamo action can be achieved by increasing the Reynolds number of the flow, and not just by changing the Prandtl number. We note here that, in the Sun,  $\text{Pr}_M$  is of the order  $10^{-7}$ , so that this mechanism cannot provide a qualitative picture of the phenomena involved there in the small scale dynamo. Moreover, whenever  $\text{Pr}_M \lesssim 1$ , the mechanism proposed here could not work because then the typical length scale for magnetic diffusion ( $\eta^3/\epsilon$ )<sup>1/4</sup> would be larger than the kinematic dissipation length so that advection of magnetic fields on the scales of the vorticity tubes would be impossible.

### IV. A COMPARISON WITH TURBULENT HYDROMAGNETIC CONVECTION DATA

We now use our vortex model of dynamo action to try to explain dynamo action seen in the numerical simulations of Brandenburg *et al.*<sup>12</sup> In those simulations, the dynamo results from turbulent convection that develops in a convectively unstable layer of depth  $L$  between two stably stratified layers. The nondimensional units used are such that length and time units are  $[x]=L$  and  $[t]=(L/g)^{1/2}$ , where  $L$  is the depth of the unstable convection zone and  $g$  is the acceleration of gravity. For further details see Ref. 12. In particular we look at snapshots of velocities from two runs, Run A and Run D, that differ from each other in resolution, Reynolds and Prandtl numbers (see Table I). Run A has a smaller Reynolds number and a larger magnetic Prandtl number than Run D.

In both cases, a turbulent magnetic field is sustained against magnetic diffusion by dynamo action. Looking at the flow pattern (Fig. 4), we can identify vortex pairs. We, therefore, measure the relevant parameters for the local magnetic Reynolds (or Herzenberg) number, as defined in Eq. (12), at the scale  $a$  of the vortex tubes and compare this value with the critical value for dynamo action as estimated in Eq. (11).

We display in Table II the measured values of the parameters for two arbitrarily chosen vortex pairs in Runs A and D. The value of  $a$  is taken to be the radius within which the vorticity exceeds three times the rms value. The value of  $\Omega$  is taken to be  $\omega_{\max}/2$ . Given the value of  $\eta$  (Table I) we find the values of Hz to be 100 and 20 for Runs A and D, respectively. The critical value, on the other hand, is around 75. Here we have assumed that  $d=a$ , which is appropriate for close vortex pairs. We have also assumed  $\phi=125^\circ$ ,

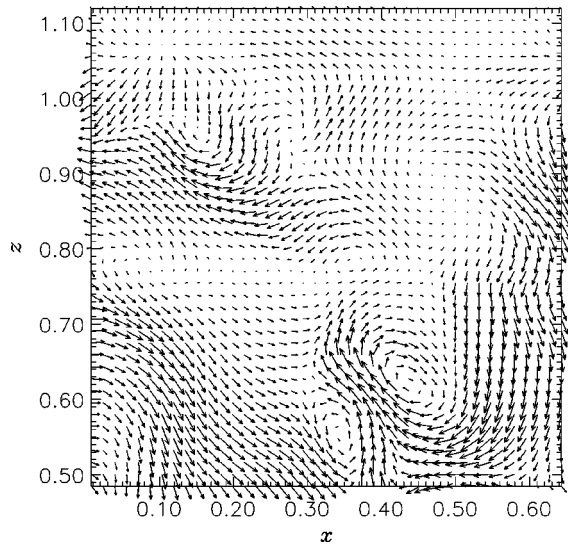


FIG. 4. Run D. Velocity vectors in a part of a  $x$ - $z$  cross section through  $y=1.03$ . The two vortices seen near the bottom are considered in the rotor model of Sec. IV.

which is the most optimistic case. However, even in that case the vortex model would still be subcritical by a factor of almost 4 when applied to Run D. Thus, although Herzenberg dynamo action is possible in case A, this is hardly a viable dynamo mechanism, because it does not work in case D, where turbulent dynamo action is also observed.

Note that, in Run D the Prandtl number is less than unity. As we have already seen at the end of Sec. III B this is an unfavorable condition for the mechanism that we have proposed to explain dynamo action. This is simply because the diffusion length of the magnetic field is now larger than the dissipation scale  $\ell$ . Thus, on the scale of the vortex tubes the magnetic Reynolds number is too small for dynamo action to be possible.

## V. ON THE SCALING OF THE RATIO $a/d$ WITH $Re$

We have seen in Eq. (11) that the critical value of  $Hz$  depends on  $(a/d)^{-2.7}$  multiplied by a number that is around 75 for  $\phi=125^\circ$ . We have so far assumed that  $(a/d)\sim 1$ . We are here interested in the possibility that this ratio depends upon the Reynolds number. On the one hand,  $a$  decreases as  $Re$  increases, but on the other, the number of vortex tubes is increased. In order to estimate the mean separation of the tubes,  $d=D/2$ , we first relate  $D$  to the number of tubes,  $N_L$

TABLE II. Parameters measured in Runs A and D and the resulting Herzenberg numbers.  $\Omega$ ,  $d$  and  $\eta$  are given in nondimensional units, where  $g=L=1$ .

	Run A	Run D
$\Omega = \omega_{\max}/2$	1	1.4
$a$	0.07	0.03
$d$	0.07	0.03
$\eta$	$5.0 \times 10^{-5}$	$6.2 \times 10^{-5}$
$Hz$ , Eq. (12)	100	20

say, in the volume  $L^3$ . This number is related to the fractional volume occupied by the tubes which in turn is related to the filling factor.

For the purpose of counting the number of tubes, we may think of all tubes being rearranged such that they are all parallel to each other and equally spaced, the distance between each tube being  $D$ . To cover the whole surface of a box of size  $L$  we need  $N_L$  tubes such that  $N_L D^2 = L^2$ . Therefore the number of those tubes is just

$$N_L = (D/L)^{-2}. \quad (21)$$

On the other hand, given the assumption about the size of such tubes, the volume of each tube is roughly

$$V \approx a^2 L, \quad (22)$$

so the number of tubes equals the total volume occupied by all tubes divided by the volume of each tube, which is  $V$ . The total volume occupied by all tubes is  $fL^3$ , where  $f$  is the filling factor. Thus, we have  $N_L V \approx fL^3$ , or

$$N_L \approx fL^3/V = f(a/L)^{-2}. \quad (23)$$

Eliminating  $N_L$  from Eqs. (21) and (23), we find that  $D = af^{-1/2}$ , or, since  $D=2d$ ,

$$a/d = 2f^{1/2}. \quad (24)$$

Thus,  $a/d$  depends on the filling factor. The value of  $f$  is not well defined, because vortex tubes do not have sharp boundaries. If we define tubes as those regions where  $|\omega|$  exceeds 25% of the maximum value, then the filling factor is 0.05 and fairly independent of resolution and Reynolds numbers.<sup>12</sup> This is because the probability density function of the vorticity is very nearly exponential. In this case not only  $f$ , but also  $a/d$  would be independent of the Reynolds number. There is however a problem, because in order to have dynamo action we would have to require, according to Eqs. (19) and (11), that  $Pr_M \geq 75f^{-1.35} \approx 6000$ . This clearly cannot explain the results of the simulations where  $Pr_M = O(1)$  (see Table I). One possible explanation is that some tubes may have much smaller separations than others, and dynamo action is mainly accomplished by a small number of close pairs of tubes. But even then  $Pr_M$  would have to exceed a value of about 70, which is not the case.

## VI. VARIATIONS ON THE MODEL

The considerations of the previous sections suggest that the hypothesis of dynamo action from interactions of pairs of vortex tubes can be rejected, if the magnetic Prandtl number is small. Many astrophysical bodies, including the Sun and other stars, have small magnetic Prandtl numbers, whereas it is generally believed that in them a small-scale dynamo does operate.<sup>22</sup> Of more immediate concern to us is the fact that in Run D, where we know that there is small-scale dynamo action, the numbers do not support the hypothesis that small-scale dynamo action is due to interaction between pairs of vortex tubes. Thus, we must look for other ways to explain this.

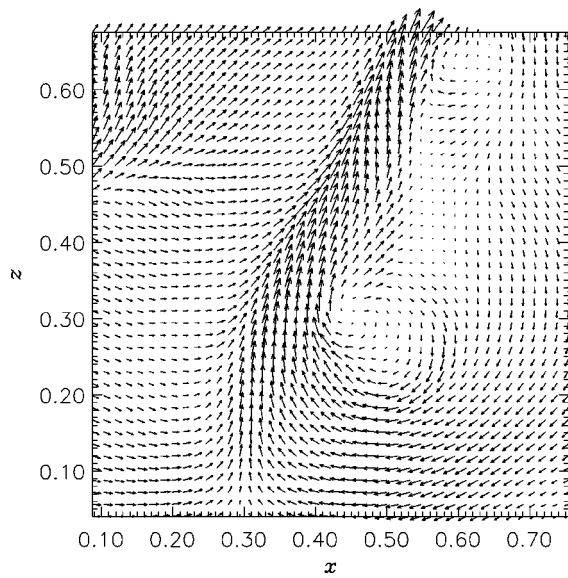


FIG. 5. Run D. A close-up of velocity vectors in a  $x-z$  cross section ( $y = 1.03$ ) showing a vortex sheet together with part of a vortex.

**A. Vortex sheets**

Closer inspection of visualizations of vorticity suggests not only the presence of vortex tubes, but also of vortex sheets due to regions of fluid moving in the form of down-drafts. An example is shown in Fig. 5, where we show a two-dimensional cross-section of the velocity field of Run D, and the corresponding magnetic field of the form shown in Fig. 6. The combined occurrence of vortex sheets and tubes has also been noted earlier.<sup>4</sup>

Although vortex sheets are probably not as prominent as tubes when visualized using a threshold procedure, they may still be important for the dynamo because of the enhanced area over which tubes interact with a sheet. We have performed a simulation relevant for this case, in a similar fashion to that used in the case of vortex tubes. We have considered a system composed of a vortex sheet and a spherical

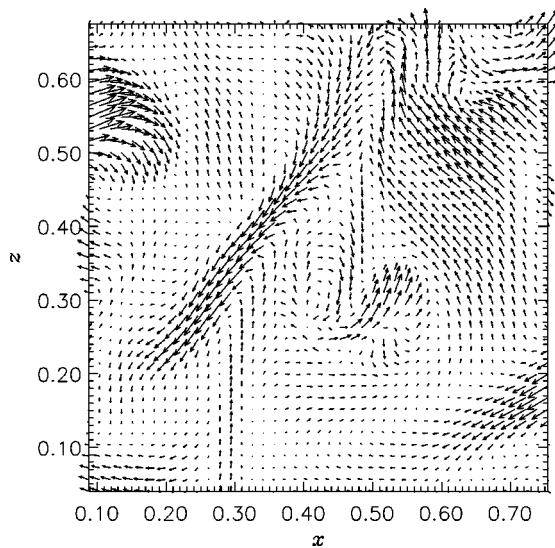


FIG. 6. Run D. Magnetic field vectors in the same cross section as in Fig. 5.

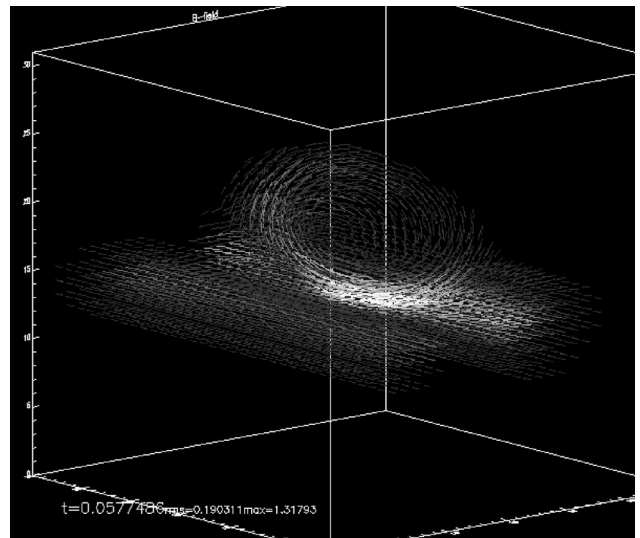


FIG. 7. The magnetic field vectors for the vortex sheet model with one rotor in a case where the dynamo is excited. Here the rotation axis of the sphere and the vorticity vector of the sheet lie in parallel planes and the two vectors are at an angle of  $\phi = 45^\circ$  to each other.

rotor of radius  $a$  whose rotation axis is inclined with respect to the direction of the vorticity vector of the sheet. The sheet is defined such that the vorticity takes the form

$$\boldsymbol{\omega} = \omega_x(z)(1,0,0), \quad \omega_x = -2\frac{u_0}{a^2}z \exp[-(z/a)^2], \quad (25)$$

with the corresponding velocity of the form  $\mathbf{u} = (0, u_y, 0)$ , where

$$u_y = u_0 \exp[-(z/a)^2]. \quad (26)$$

The rotor is placed a distance  $d = a$  from the sheet.

For such a system, we can define a modified Herzenberg number  $\widetilde{\text{Hz}}$  as the geometrical mean of the relevant magnetic Reynolds numbers for the rotor and the sheet,

$$\widetilde{\text{Hz}} = \left[ \left( \frac{Ua}{\eta} \right) \left( \frac{\Omega a^2}{\eta} \right) \right]^{1/2}. \quad (27)$$

The growth rate of the magnetic field depends on the relative orientation of the rotation axis of the rotor and the vorticity vector of the sheet, and can be positive. In our most favorable case, when the two vectors lie in two parallel planes with relative angle  $\phi = 45^\circ$ , the critical value is

$$\widetilde{\text{Hz}}_{\text{crit}} = 30. \quad (28)$$

(Note that, for  $\phi = 135^\circ$ , for example, we found no dynamo action.) The structure of the magnetic field resulting from dynamo action for  $\phi = 45^\circ$  is shown in Fig. 7. The relevant parameters are  $U = 0.08$ ,  $a = 0.05$ ,  $\Omega = \omega/2 = 1.5$  and  $\eta = 6.2 \times 10^{-5}$ . Making use of the definition (26) and measuring the parameters at an arbitrarily chosen location in Run D, we find that  $\widetilde{\text{Hz}}_{\text{Run D}} \approx 60$ , which is twice the critical value. We thus conclude that this vortex sheet model could possibly contribute to dynamo action in Run D.

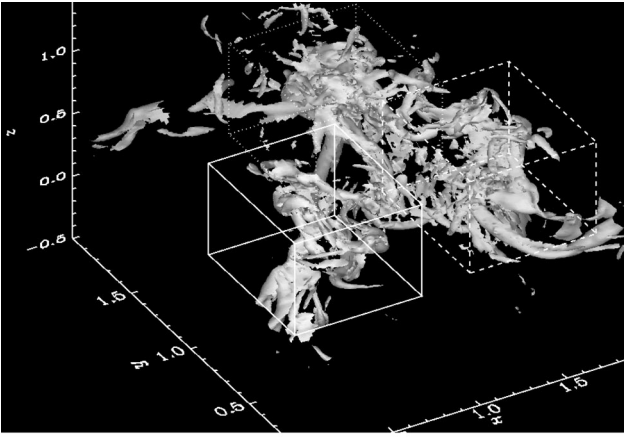


FIG. 8. Three dimensional visualization of the level surface of the vorticity in Run D, where its value is 25% of the maximum. Three vortex clusters may be identified; see the three subvolumes (solid, dotted, and dashed lines).

### B. Vortex clusters: A three rotor dynamo

Another possibility for explaining dynamo action in Run D is that dynamo action occurs *not* on the smallest possible scale, the diameter of tubes, but on larger scales (either in addition, or solely). The power spectrum of the magnetic field supports the view that the magnetic energy contains contributions from all scales.<sup>12</sup> A close inspection of the vorticity field in Run D suggests that the tubes group into two or three distinct clusters (see Fig. 8).

Clusters are in relative motion to each other and so this raises the question whether each cluster could be considered as a “super-rotor.” In the following we consider this suggestion quantitatively. Looking at visualizations of the vorticity (Fig. 8) of Run D we identify three distinct clusters, where many vortex tubes accumulate. We construct from each cluster the mean vorticity vector  $\langle \boldsymbol{\omega} \rangle_i$ ,  $i = 1, 2, 3$ , that we take in the form

$$\langle \boldsymbol{\omega} \rangle_i = \omega_i \begin{pmatrix} \sin \vartheta_i \cos \varphi_i \\ \sin \vartheta_i \sin \varphi_i \\ \cos \vartheta_i \end{pmatrix}, \quad (29)$$

where  $\vartheta$  and  $\varphi$  are polar angles of  $\langle \boldsymbol{\omega} \rangle$  with respect to the vertical axis and  $i = 1, 2, 3$  is a label for the three subvolumes encompassing the three vortex clusters. The definition of the boundaries of the subvolumes is somewhat arbitrary and we have therefore considered different possibilities. Numerical values are given in Table III for one particular choice.

TABLE III. Spherical coordinates of the averaged vorticity vectors for the three rotor model of the dynamo. The values of the individual nondimensional numbers that occur in the formula for the magnetic Reynolds number  $\text{Hz}$  of the system are also given. We used  $\eta = 6.18 \cdot 10^{-5}$ ,  $a = 0.37$ .

$i$	$\omega_i$	$\vartheta_i$	$\varphi_i$	$\omega_i a^2 / 2\eta$
1	0.06	75°	-90°	66
2	0.03	91°	126°	33
3	0.03	116°	-179°	33

TABLE IV. Critical Herzenberg number  $\text{Hz}_{\text{crit}}$  for the three rotor system obtained from the numerical simulations. Three different configurations for the boxes have been considered.

Configuration	$a$	$\text{Hz}_{\text{crit}} / \text{Hz}_{\text{Run D}}$
(i)	0.37	4.1
(ii)	0.27	3.1
(iii)	0.32	2.7

Due to mutual cancellations of nearly anti-aligned pairs of vortex tubes the magnitude of the averaged vorticity is smaller than the vorticity in the small individual vortex tubes considered so far (see, e.g., Table II). Quantitatively, this can be described considering the velocity structure function,

$$\delta u_r = U(r/L)^{1/3}, \quad (30)$$

where  $\delta u_r$  is the transversal velocity difference between two points separated by a distance  $r$ . The vorticity over a scale  $r$  is then

$$\omega_r = \delta u_r / r = (U/L)(r/L)^{-2/3}. \quad (31)$$

The vorticity on a length scale of the order of the integral scale  $L$  is just  $U/L$ . Using the data from Table I we have  $U/L = 0.036$ , which is consistent with the value given for  $\omega_i$  in Table III. On the other hand, making use of (31), we see that the numerical value of the vorticity on the scale  $a = 0.02L$  (which is the scale of the vortex tubes in Run D) is around one. This is consistent with the direct measurement of the value of  $\omega$  for Run D (see Table II).

We now use the three vorticity vectors obtained above to construct a system of three spherical rotors in which the angular velocities of the rotors  $\boldsymbol{\Omega}_i$  is such that  $\boldsymbol{\Omega}_i = \langle \boldsymbol{\omega} \rangle_i / 2$ . For this system of vortex clusters we define a Herzenberg number  $\text{Hz} = \Omega a^2 / \eta$ , where now  $a$  is the size of the cluster and  $\Omega$  is the geometric mean of the moduli of the angular velocities of the three rotors. In order to test the sensitivity of the model to the choice of the boxes, we have performed the simulations for three different choices of the dimensions and location of the clusters. The critical value for the magnetic Reynolds numbers  $\text{Hz}_{\text{crit}}$  for these three different cases are given in Table IV and they are compared with the critical values calculated for the Run D. We can see that the three rotor models are still subcritical by approximately a factor three.

Instead of taking volume averages, we could have taken averages over shells of different thickness. This, however, does not seem to change the qualitative results that we have obtained with the full boxes. A comparison between different averaging procedures is given in Table V. From those results we may conclude that the vortex cluster model cannot explain the dynamo action present in Run D.

In summary, among the variations on the model the vortex sheet model gives dynamo action for the smallest magnetic Reynolds number.

### VII. IS TIME DEPENDENCE IMPORTANT?

It is possible that a flow field that is evolving in time may accelerate the transport of field between rotors. In the

TABLE V. The components of the averaged vorticity vector when the averaging is carried out over spheres and shells of different radii (given as numbers of mesh points).

$r_{\text{ext}}$	$r_{\text{int}}$	$\omega$	$\vartheta$	$\varphi$
14	0	0.48	59	40
17	0	0.38	49	44
28	0	0.078	61	32
14	12	0.46	52	57
17	16	0.32	33	57
28	13	0.12	50	70

traditional Herzenberg dynamo this is accomplished by diffusion, which is a slow process. One could therefore imagine that field advection (instead of field diffusion) between the two rotors could facilitate dynamo action. In order to clarify this we now present the results of a kinematic calculation using a frozen-in-time velocity field taken from the same snapshot of Run D for which the vorticity is given in Fig. 8. The numerical resolution is  $126 \times 126 \times 105$  meshpoints, which is identical to that of the original convection simulations.

We find that, even in the kinematic case, the magnetic field organizes itself in the form of flux tubes (see Fig. 10). Note that in order to see those structures, we have lowered the level of the contour shown in this figure to only 7% of the maximum value. (At 18% of the maximum, i.e., the value used in Fig. 11, only a single spot would have been visible. Thus the field is much more strongly localized in the kinematic case.) In Fig. 9 we show the growth of the magnetic energy as a function of time for two different values of  $1/\eta$  ( $\sqrt{gL^3}/\eta$  in dimensional units). For  $1/\eta = 2 \times 10^4$ , corresponding to a magnetic Reynolds number of about 700, we found a growth rate of about 3200 inverse diffusion times, corresponding to an  $e$ -folding time of about 0.2 turnover times. For  $1/\eta = 10^4$  (magnetic Reynolds number about 350) we found a growth rate of about 170 inverse diffusion times, corresponding to an  $e$ -folding time of about 6 turnover times. Extrapolating on these two cases we expect the critical value of  $1/\eta$  for dynamo action to be just below  $10^4$ . In both cases

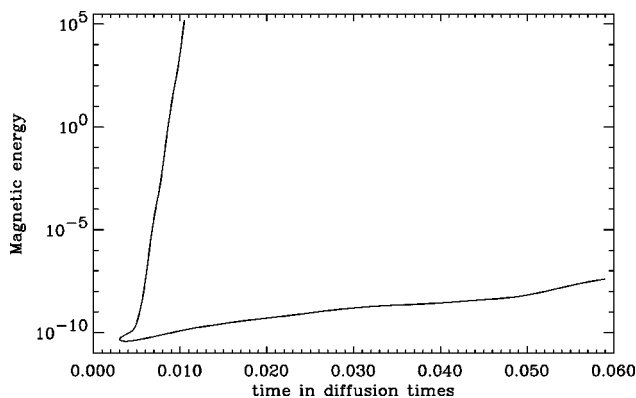


FIG. 9. The dependence of magnetic energy on time in a kinematic calculation using a frozen-in-time velocity field taken from Run D. Two cases are plotted; one where the velocity was 18% larger than in the original dynamical calculation ( $1/\eta = 2 \times 10^4$ ; upper curve) and one where it was only 60% of the original value ( $1/\eta = 10^4$ ; lower curve).

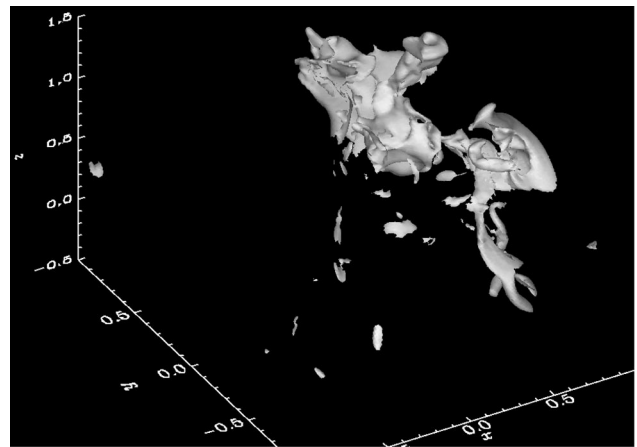


FIG. 10. Three dimensional visualization of the level surface of the magnetic field in the kinematic calculation using a frozen-in-time velocity field taken from Run D. The value of the level surface is 7% of the maximum field strength. The time is the same as in the vorticity plot in Fig. 8. Note the concentration of field into structures.

the growth is oscillatory. The value of  $1/\eta$  used in the original dynamical calculation was  $1.6 \times 10^4$ . The fact that dynamo action is found even for a time independent flow field suggests that time dependence is not essential for turbulent dynamo action. Moreover, even for  $1/\eta = 10^4$  the growth time was shorter (6 turnover times) than in the dynamical calculation with  $1/\eta = 1.6 \times 10^4$ , where the growth time was about 20 turnover times. Hence, in an evolving velocity field the magnetic field growth is actually slower.

For comparison, we show in Fig. 11 a snapshot of the magnetic field configuration from Run D at the instant at which we took our kinematic velocity field. When compared with Fig. 10, there are some broad similarities, but also obvious differences. In particular, there is a strong ‘hot-spot’ in Fig. 10, which is only marginally present in Fig. 11. The explanation seems reasonably straightforward. The growth time for the dynamo is considerably greater than the characteristic time scale of the dynamically driven motions of Run D. Thus, in this case, there is never enough time for the

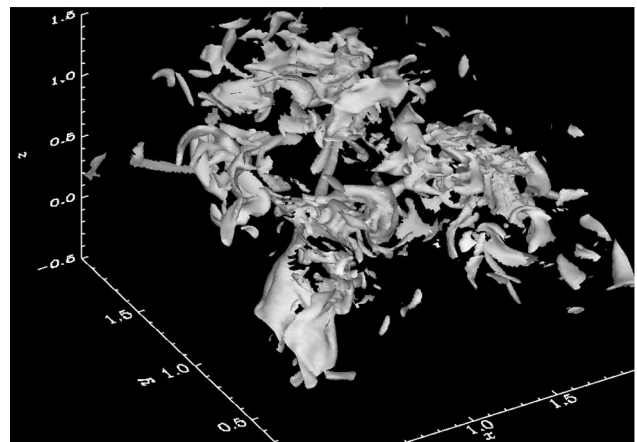


FIG. 11. Three dimensional visualization of the level surface of the magnetic field in the dynamical simulation of Run D. The value of the level surface is 18% of the maximum field strength. The time is the same as in the vorticity plot in Fig. 8.

magnetic field to approach the steadily growing (instantaneous) eigenmode, which is illustrated in Fig. 10. (This also plausibly explains why the evolving velocity field gives a slower growth rate for the magnetic field.) These comparisons provide at least a hint that, although a time invariant “frozen” velocity field can support a dynamo, it may not be a valid way to investigate time dependent dynamo action.

A comparable difference between “frozen” and evolving velocity fields has also been seen in particle advection by turbulent flows.<sup>23</sup> There, with the “frozen” velocity field, particles continue to stream into the same points, while in the time-dependent case such points are never sufficiently long lived for this to happen. On the other hand, statistical properties such as topological entropies are remarkably similar in the two cases.<sup>24</sup> This suggests that the complicated nature of the velocity field (see, e.g., Fig. 8) is an important property of the dynamo, which is difficult to model by a constructed flow field such as the simple vortex model considered here.

### VIII. CONCLUSIONS

The present calculations have shown that a vortex pair or cluster model can produce dynamo action with parameters appropriate to the simulation with  $Pr_M=4$  (Run A), but not for parameters chosen to represent the simulation with  $Pr_M=0.5$  (Run D). Given that the original convection simulations did exhibit dynamo action in both cases, we must conclude that our simple vortex models cannot be viable — at least not for low values of  $Pr_M$ . There are several possible reasons. If we look at, for example, Fig. 4, we see that the two vortices that we model occupy a small fraction of the computational domain. It could be imagined that local Herzenberg-type amplification of magnetic field might occur in the vicinity of these vortices, but in a simple model (Sec. IV), much of the toroidal (with respect to the vortex axes) flux generated will diffuse to large distances, whilst decaying. For the adopted vortex parameters, a dynamo is not maintained. In the presence of the complete velocity field, other vortices, either singly or in groups, will interact with and amplify this diffusing field. (We do not suggest that this secondary process need itself constitute dynamo action, merely field amplification.) Some of this amplified field will then diffuse back towards the original vortex pair. This influx of magnetic field could take a nominally subcritical Herzenberg-type system into a supercritical regime. In this sense, dynamo action would be a collective phenomenon, which cannot be analyzed locally.

Another possibility is that large scale motions not associated directly with the vortex tubes play a vital role in exciting the dynamo, perhaps by enhancing the transport of

magnetic flux between vortices. More generally, and in some ways encompassing both of these points, we might say that turbulent motions occur on a large range of length scales and that essential contributions to dynamo action come from motions on larger scales. The geometry of the velocity field for a working dynamo is clearly very complex (see Fig. 8) and plausibly cannot easily be described by a simple vortex model, which only mimics selected local features of the flow field.

### ACKNOWLEDGMENTS

We thank Anvar Shukurov for stimulating discussions and useful comments on the manuscript. We also thank an anonymous referee for his/her suggestions that have helped to improve the presentation.

This work was supported in part by the European Community Human Capital and Mobility (Networks) project “Late type stars: Activity, magnetism, turbulence” No. ERBCHRXCT940483.

<sup>1</sup>E. D. Siggia, *J. Fluid Mech.* **107**, 375 (1981).

<sup>2</sup>R. M. Kerr, *J. Fluid Mech.* **153**, 31 (1985).

<sup>3</sup>A. Vincent and M. Meneguzzi, *J. Fluid Mech.* **225**, 1 (1991).

<sup>4</sup>H. K. Moffatt, S. Kida, and K. Ohkitani, *J. Fluid Mech.* **259**, 241 (1994).

<sup>5</sup>U. Frisch, *Turbulence: The Legacy of A. N. Kolmogorov* (Cambridge University Press, Cambridge, 1995), pp. 125 and 184.

<sup>6</sup>S. I. Vainshtein and Ya. B. Zeldovich, *Sov. Phys. Usp.* **15**, 159 (1972).

<sup>7</sup>A. P. Kazantsev, *Sov. Phys. JETP* **26**, 1031 (1968).

<sup>8</sup>M. Meneguzzi, U. Frisch, and A. Pouquet, *Phys. Rev. Lett.* **47**, 1060 (1981).

<sup>9</sup>M. Meneguzzi and A. Pouquet, *J. Fluid Mech.* **205**, 297 (1989).

<sup>10</sup>S. Kida, S. Yanase, and J. Mizushima, *Phys. Fluids A* **3**, 457 (1991).

<sup>11</sup>Å. Nordlund, A. Brandenburg, R. L. Jennings, M. Rieutord, J. Ruokolainen, R. F. Stein, and I. Tuominen, *Astrophys. J.* **392**, 647 (1992).

<sup>12</sup>A. Brandenburg, R. L. Jennings, Å. Nordlund, M. Rieutord, R. F. Stein, and I. Tuominen, *J. Fluid Mech.* **306**, 325 (1996).

<sup>13</sup>A. Brandenburg, D. Moss, and A. M. Soward, *Proc. R. Soc. London, Ser. A* **454**, 1283 (1998).

<sup>14</sup>A. Herzenberg, *Philos. Trans. R. Soc. London, Ser. A* **250**, 543 (1958).

<sup>15</sup>F. J. Lowes and I. Wilkinson, *Nature (London)* **198**, 1158 (1963).

<sup>16</sup>H. K. Moffatt, *Magnetic Field Generation in Electrically Conducting Fluids* (Cambridge University Press, Cambridge, 1978), p. 122.

<sup>17</sup>R. D. Gibson, *Q. J. Mech. Appl. Math.* **21**, 243 (1968).

<sup>18</sup>S. K. Lele, *J. Comput. Phys.* **103**, 103 (1992).

<sup>19</sup>J. M. Hyman, *A Method of Lines Approach to the Numerical Solution of Conservation Laws*, in: *Advances in Computation Methods for Partial Differential Equations*, edited by R. Vichnevetsky and R. S. Stepleman (International Association for Mathematics and Computers in Simulation, New Brunswick, NJ, 1979), Vol. III, pp. 313–343.

<sup>20</sup>A. Brandenburg, I. Procaccia, and D. Segel, *Phys. Plasmas* **2**, 1148 (1995).

<sup>21</sup>G. K. Batchelor, *Philos. Trans. R. Soc. London, Ser. A* **201**, 405 (1950).

<sup>22</sup>S. Childress and A. G. Gilbert, *Stretch, Twist, Fold: the Fast Dynamo* (Springer, Berlin, 1995), p. 4.

<sup>23</sup>L. S. Hodgson and A. Brandenburg, *Astron. Astrophys.* **330**, 1169 (1998).

<sup>24</sup>A. Brandenburg, I. Klapper, and J. Kurths, *Phys. Rev. E* **52**, R4602 (1995).